

Direct observation of discommensurate walls in Bi-Ca-Sr-Cu-O superconductors

J.-W. Lee and D. E. Laughlin

Department of Metallurgical Engineering and Materials Science, Carnegie Mellon University, Pittsburgh, Pennsylvania 15213

S. Nam

*University Research Center, Wright State University, Dayton, Ohio 45435
and WRPC/POOC, Bldg. 450, Wright-Patterson Air Force Base, Ohio 45433*

(Received 8 September 1989)

The dislocations and twins in superconducting Bi-Ca-Sr-Cu-O samples are examined by scanning electron microscopy and transmission electron microscopy. The results indicate that these defects are inherent to the materials. The grains are large in size (1–10 μm), but they are frequently divided into subgrains by low-angle grain boundaries. Furthermore, evidence is found for discommensurate walls associated with incommensuration along the b axis.

INTRODUCTION

Since the discovery of high- T_c superconductors La-Ba-Cu-O (Ref. 1) and Y-Ba-Cu-O (Ref. 2), many other oxides have shown superconductivity at high temperature: e.g., Bi-Ca-Sr-Cu-O,³ Tl-Ba-Ca-Cu-O,⁴ and Ba-K-Bi-O.⁵ Among these, Bi-Ca-Sr-Cu-O superconductors ($T_c \approx 85$ and 110 K) have drawn much attention since they provide high T_c and are easier and cheaper to fabricate than the others. It is known, however, that these materials exhibit incommensurate superstructures along the b axis in the orthorhombic phase and that the materials are composed of both low- and high- T_c superconducting phases. Direct observation of the incommensuration by electron diffraction is abundant in the literature.^{6–11} However, the origin and nature of the incommensuration is not known yet, although several explanations have been proposed. These include clustering of Sr and oxygen vacancies,⁶ occupational and/or positional fluctuation of Bi sites in the Bi_2O_2 layer,⁷ the aperiodic replacement of Bi by Cu,¹² and the presence of antiphase boundaries.¹³

Many investigators have tried to single out the low- and high- T_c superconducting phases. Identification of

the low- T_c phase (85 K) was successful in Ref. 14. This phase has lattice parameters: $a \approx 0.54$ nm, $b \approx 5a$, and $c \approx 4\sqrt{2}a$. However, the crystallographic details of the high- T_c phase (110 K) are still under investigation, although the high- T_c phase is known to have a tetragonal structure ($a \approx 0.54$ nm and $c \approx 3.7$ nm).¹⁵ Thus, the objective of this work is to examine the microstructural details of Bi-Ca-Sr-Cu-O superconductors utilizing transmission electron microscopy (TEM). Special attention is given to the characterization of the nature of the incommensurate superstructures as well as the presence of other defects.

EXPERIMENTAL

Samples were prepared by solid-state reaction from powders CaCO_3 , SrCO_3 , Cu_2O , and Bi. Three nominal compositions were prepared: $\text{BiSrCaCu}_2\text{O}_x$ with (A) and/or without (B) Pb in trace amounts and $\text{BiSrCaCu}_3\text{O}_x$ (C), respectively. The magnetization of samples was reported previously.¹⁶ Specimens for scanning electron microscopy (SEM) were prepared by



FIG. 1. SEM micrograph of fractured sample B.



FIG. 2. BF image of sample A (zone axis (z) = near[001]).

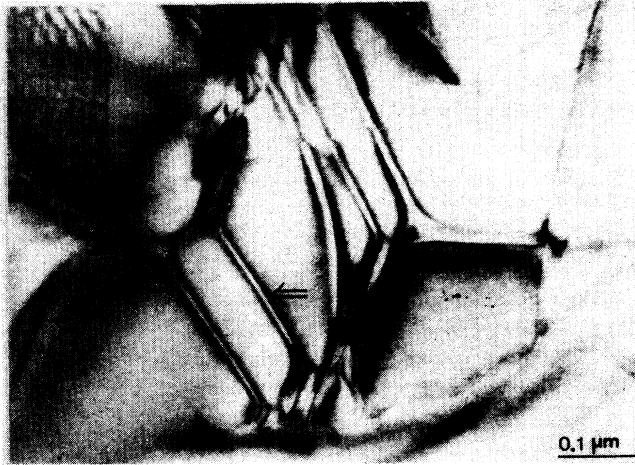


FIG. 3. BF image of sample C.

fracturing the sintered samples. SEM examination was conducted in a CamScan Series 4 operating at 35 kV.

For TEM, the sintered samples were ground in an agate mortar and pestle and collected on carbon coated copper grids. Ion milling was done on mechanically ground samples. TEM was performed using a Philips EM 420 T analytical electron microscope operating at 120 kV using both room temperature and liquid-nitrogen cold stages. The crystallographic orientation and lattice constants of the samples were determined using a combination of selected-area-diffraction (SAD) and convergent-beam electron-diffraction (CBED) patterns.

Additionally, bright/dark field (BF/DF) imaging modes were utilized along with high-resolution electron microscopy (HREM).

RESULTS AND DISCUSSION

The morphology of the superconductors was investigated on fractured samples by SEM. A typical example is shown in Fig. 1 (sample B). One can see a steplike morphology. This indicates that the materials are layered and that the fracture occurs on a specific family of planes. Platelets of approximately 10 μm in size can be seen. However, this does not correspond to the grain size, since these platelets often contain several grains.

Almost all the crystal fragments on the carbon-coated Cu grids reveal grains with the [001] zone axis. This indicates that (001) is a cleavage plane for this material.¹⁷ Such cleavage planes are shown in the steplike morphology in SEM images (see Fig. 1).

In general, it is not easy to get good CBED patterns in these specimens. This is most likely due to strains present in the materials and contamination by electron beam heating. The presence of strains can be confirmed by the observation of defects such as twins, dislocations, and a large amount of bend contours (see Fig. 2). These defects can be introduced by mechanical damage during specimen preparation for TEM. However, ion milled specimens show them to be present as well. We conclude that they are inherent to the materials.

The grain size of these materials is large (up to 10 μm), although small grains (50–100 nm) are infrequently ob-

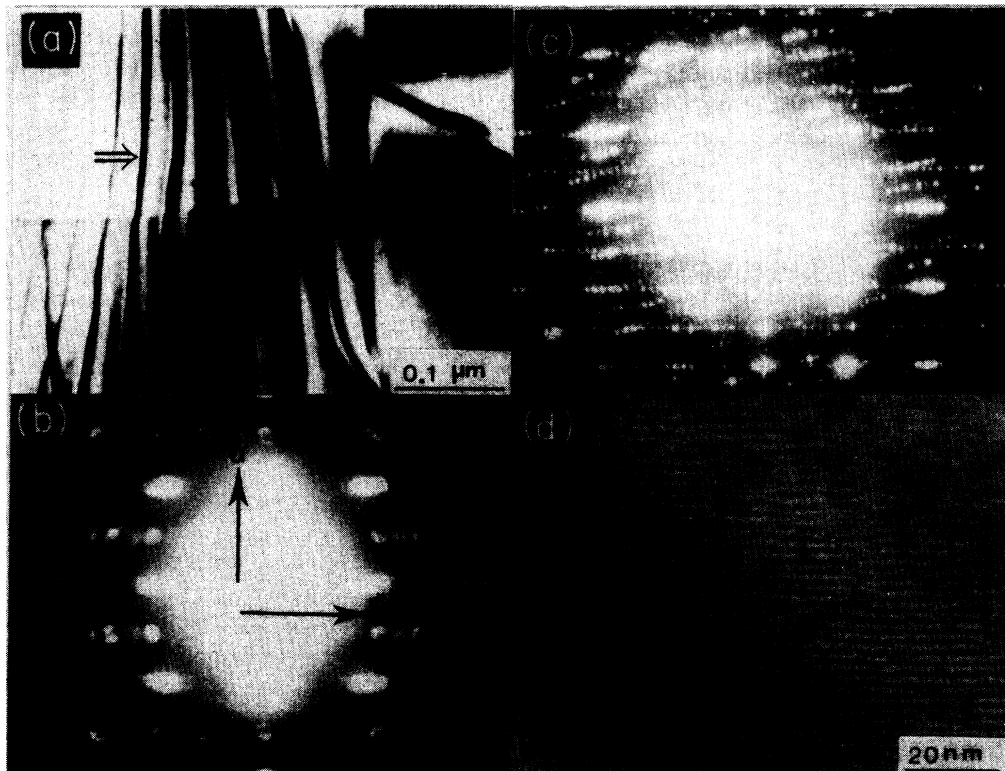


FIG. 4. BF image of sample B (a) together with its CBED (b) and SAD (c) patterns as well as Moire image of a stripelike line (d).

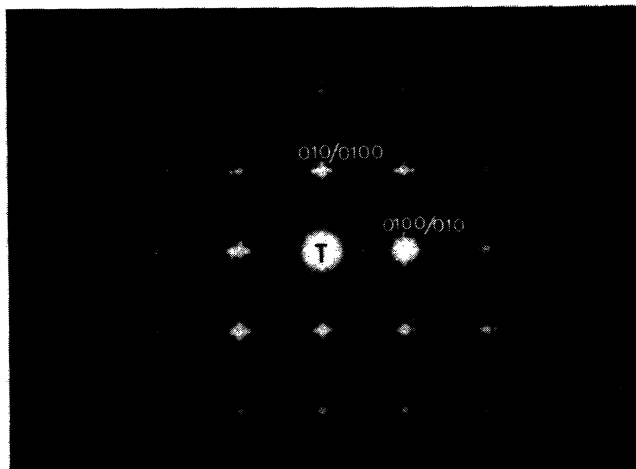


FIG. 5. A representative SAD pattern for a 90° twist boundary on sample C.

served in sample A. The large grains are generally fragmented by stripelike lines as observed in Ta_2O_5 (Ref. 18) [see arrows in Figs. 3 and 4(a)]. The lines often form networks (Fig. 3) and are found to be low-angle boundaries ($< 1^\circ$) by CBED patterns [Fig. 4(b)]. This can be further confirmed by SAD using a larger aperture [Fig. 4(c)]

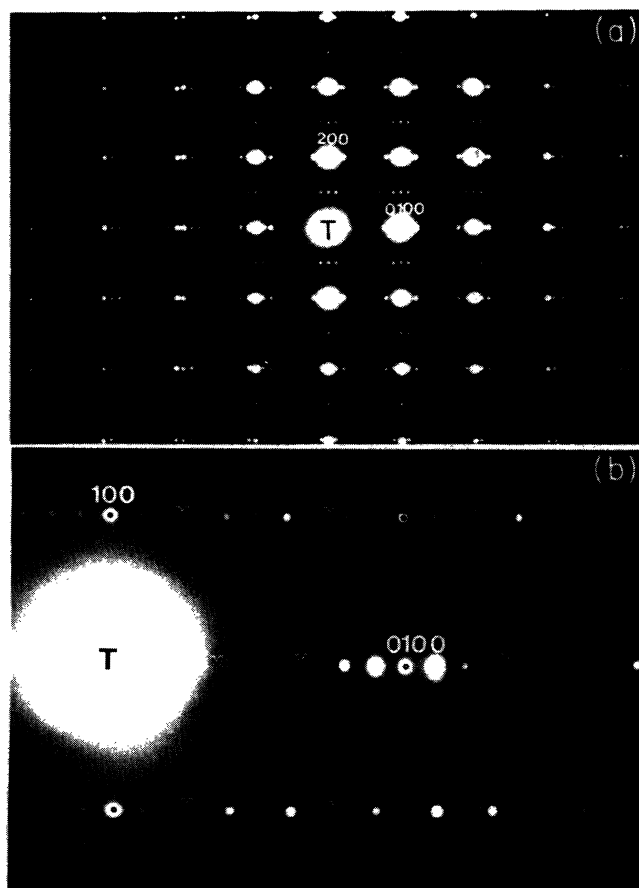


FIG. 6. SAD pattern of sample C (z =near $[001]$) (a), together with its enlarged pattern (b).

where several superimposed $[001]$ zone axes can be seen. Higher magnification of the regions delineated by the stripelike lines reveals rotational Moiré fringes [Fig. 4(d)]. The calculated angle of rotation is consistent with the value observed by diffraction.

As observed by other investigators, we found a 90° twist boundary where the a and b axes are interchanged (see Fig. 5). The twisted plane is perpendicular to the $[001]$ zone axis. This can occur since the lattice parameters of the samples in the a and b direction are nearly equal for the basic unit cell. However, it should be noted that this diffraction pattern was obtained on a single grain as confirmed by microdiffraction (probe size < 3 nm). Furthermore, the diffraction pattern reveals extra peaks due to double diffraction as is observed in overlapping crystals. Therefore, we can conclude that the pattern arises from a region where the twist boundary is in the plane of the thin film.¹⁰

Figure 6 is a typical $[001]$ diffraction pattern. This pattern consists of fundamental spots with $d_{200} \approx d_{0100}$. The reflections along the b axis are divided into 10 "superlattice or satellite" spots due to a long period modulated structure [Fig. 6(a)]. The intensity of the superlattice or satellite spots varies in a periodic way. The intense spots are grouped around the position of the fundamental

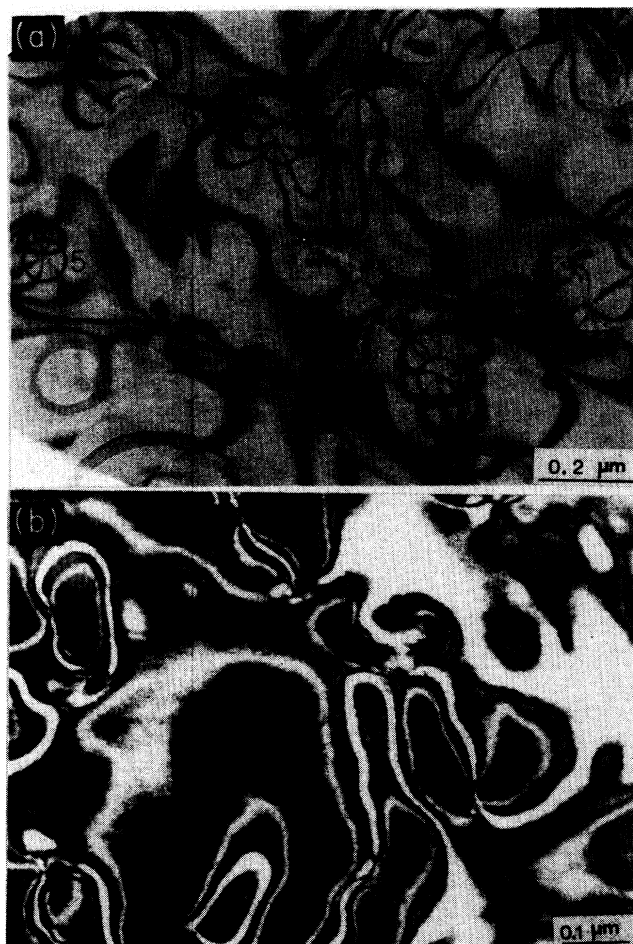


FIG. 7. BF (a) and DF (b) images of sample C, which were obtained at z =near $[001]$.

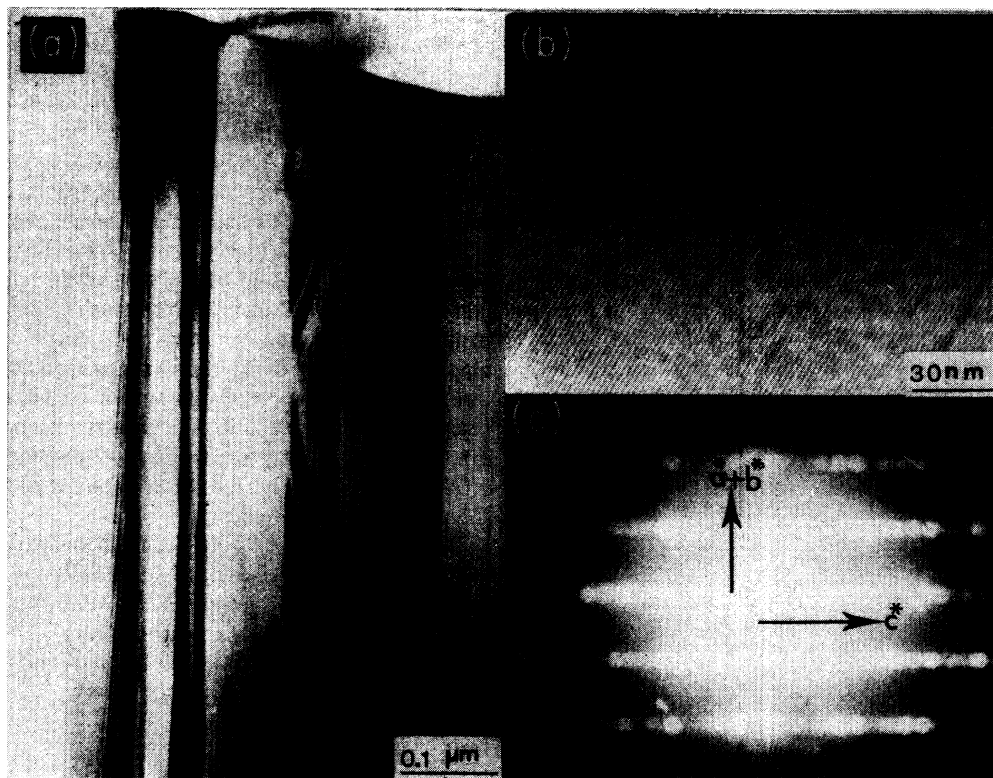


FIG. 8. BF image of twins (a) on sample C together with its HREM image (b) and SAD pattern ($z \approx [5\ 10\ 0]$) (c).

reflections of the basic unit cell, but the other superlattice reflections show up quite weakly. Van Tendeloo *et al.*¹⁹ have suggested that the rapid decrease in intensity of the satellite spots is due to a combination of an inclination of the linear sequence with respect to the (001) plane and the increasing order of the satellites. The specimens were tilted away from the exact [001] zone axis to excite the weak superlattice reflections [Fig. 6(b)]. From Fig. 6(b), it is apparent that the spacing of the superlattice reflections in the \mathbf{b}^* direction is incommensurate. This is true for all three specimens. The incommensurate spacing of the superlattice spots appears in a periodic way [see the arrows in Fig. 6(b)]. The spacings denoted by the arrows are slightly larger than $5\sqrt{2}a_p$, whereas the spacings between reflection not marked by arrows are slightly smaller than $5\sqrt{2}a_p$. Here, a_p is the perovskite lattice parameter $a_p = 0.38$ nm. Thus, every third and eighth superlattice reflection is distorted in the \mathbf{b}^* direction.

Figure 7 consists of a TEM BF (a) and DF (b) image revealing black and white regions and dark wavy lines. These images are very similar to the discommensurate walls observed in incommensurate compounds.^{20–22} We assume that the lines are discommensurate walls that bound commensurate regions.^{23,24} Discommensurate walls are supposed to appear only in the DF image using incommensurate satellite spots. It should be noted, however, that our objective aperture is large enough to encompass the incommensurate spots when placed around the direct beam (near [001] zone axis). Thus, we can see

the discommensurate walls even in the BF image. In addition, we observe either four, five, or six lines joining together to form nodes [see circles in Fig. 7(a)]. These nodes are called dislocations of the discommensurate lattice.²⁵ These dislocations and discommensurate walls are only observed when the incommensurate superlattice reflections are strongly excited. This occurs when the specimen is slightly off the exact zone axis. Thus we can conclude that the presence of the walls is responsible for incommensurate satellite spots in the \mathbf{b}^* direction of the superconductors.²⁶ There is some indication that charge-density waves (CDW) may be responsible for incommensuration and therefore of the discommensurate walls. For example, Onoda *et al.*²⁷ suggested that the larger lattice parameters in Bi-La-Sr-Cu-O superconductor arise from CDW formation. Meanwhile, Krakauer *et al.*²⁸ suggested the formation of CDW in Bi-O plane of Bi-Ca-Sr-Cu-O, but did not relate the CDW to incommensuration.

Figure 8 is a TEM image of twins. The observation of twins is not a frequent occurrence in these materials. In Fig. 8(b), each of the lattice fringes corresponding to ≈ 1.5 nm (002) are shown, but some of the fringes are distorted. This indicates that there are stacking errors of the atomic planes along the c axis. The twins are observed in the [510] zone axis [Fig. 8(c)]. The observation of twins has been reported by others²⁹ but the determination of twin plane as (510) and the reasoning for the formation of twins are not certain yet.

In conclusion, we have shown for the first time that discommensurate walls are present in the Bi-Ca-Sr-Cu-O superconductors (Fig. 7). We believe that the strain is accommodated by the formation of discommensurate walls. The grain size is large but the grains are divided by low-angle boundaries ($< 1^\circ$).

ACKNOWLEDGMENTS

This research was funded in part by the Magnetic Materials Research Group at Carnegie Mellon University under National Science Foundation (NSF) Grant No. DMR-8613386.

- ¹J. G. Bednorz and K. A. Muller, *Z. Phys. B* **64**, 189 (1986).
- ²M. K. Wu, J. R. Ashburn, C. J. Torng, P. H. Hor, R. L. Meng, L. Gao, Z. J. Huang, Y. Q. Wang, and C. W. Chu, *Phys. Rev. Lett.* **58**, 908 (1987).
- ³H. Maeda, Y. Tanaka, M. Fukutomi and T. Asano, *Jpn. J. Appl. Phys.* **27**, L209 (1988); C. W. Chu, J. Bechtold, L. Gao, Z. J. Huang, R. L. Meng, Y. Y. Sun, Y. Q. Wang, and Y. Y. Xue, *Phys. Rev. Lett.* **60**, 941 (1988).
- ⁴Z. Z. Sheng and A. M. Hermann, *Nature* **332**, 55 (1988); Z. Z. Seng, A. M. Herman, A. El Ali, C. Almasan, J. Estrada, T. Datta, and R. J. Matson, *Phys. Rev. Lett.* **60**, 937 (1988).
- ⁵R. J. Cava, B. Batlogg, J. J. Krajewski, R. Farrow, L. W. Rupp, Jr., A. E. White, K. Short, W. F. Peck, and T. Kometani, *Nature* **332**, 814 (1988).
- ⁶Y. Bando, T. Kijima, Y. Kitami, J. Tanaka, F. Izumi, and M. Yokoyama, *Jpn. J. Appl. Phys.* **27**, L358 (1988).
- ⁷Y. Matsui, H. Maeda, Y. Tanaka, and S. Horiuchi, *Jpn. J. Appl. Phys.* **27**, L361 (1988).
- ⁸H. Maeda, Y. Tanaka, M. Fukutomi, T. Asano, K. Tokano, H. Kumakura, M. Uehara, S. Ikeda, K. Ogawa, S. Horiuchi, and Y. Matsui, *Physica* **153-155C**, 602 (1988).
- ⁹E. A. Hewat, M. Dupuy, P. Bordet, J. J. Capponi, C. Chaillout, J. L. Hodeau, and M. Morezio, *Nature* **333**, 53 (1988); E. A. Hewat, P. Bordet, J. J. Capponi, C. Chaillout, J. L. Hodeau, and M. Morezio, *Physica* **153-159C**, 619 (1988).
- ¹⁰J. L. Tallon, R. G. Buckley, P. W. Giberd, M. R. Presland, I. W. M. Brown, M. E. Bowden, L. A. Christian, and R. Goguel, *Nature* **333**, 153 (1988).
- ¹¹C. H. Chen, D. J. Werder, S. H. Liou, H. S. Chen, and M. Hong, *Phys. Rev. B* **37**, 9834 (1988).
- ¹²T. Kajitani, K. Kusaba, M. Kikuchi, N. Kobayashi, Y. Syono, T. B. Williams, and M. Hirabayashi, *Jpn. J. Appl. Phys.* **27**, L587 (1988).
- ¹³R. Herrera, J. Reyes-Gasga, P. Schabes-Retchkiman, A. Gomez, and M. J. Yacaman, *Physica* **158C**, 490 (1989).
- ¹⁴K. Kugimiya, S. Kawashima, O. Inoue, and S. Adachi, *Appl. Phys. Lett.* **52**, 1895 (1988).
- ¹⁵E. Takayama-Muromachi, Y. Uchida, Y. Matsui, M. Onoda, and K. Kato, *Jpn. J. Appl. Phys.* **27**, L556 (1988).
- ¹⁶S. Nam, *Physica* **153-155C**, 316 (1988).
- ¹⁷R. M. Hazen, C. T. Prewitt, R. J. Angel, N. L. Ross, L. W. Finger, C. G. Hadjidakos, D. R. Veblen, P. J. Heaney, P. H. Hor, R. L. Meng, Y. Y. Sun, Y. Q. Wang, Y. Y. Xue, Z. J. Huang, L. Gao, J. Bechtold, and C. W. Chu, *Phys. Rev. Lett.* **60**, 1174 (1988).
- ¹⁸J. Spyridelis, P. Delavignette, and S. Amelinckx, *Phys. Status Solidi* **19**, 683 (1967).
- ¹⁹G. Van Tendeloo, H. W. Zandbergen, and S. Amelinckx, *Solid State Commun.* **66**, 927 (1988).
- ²⁰K. K. Fung, S. McKernan, J. W. Steeds, and J. A. Wilson, *J. Phys. C* **14**, 5417 (1981).
- ²¹C. H. Chen, J. M. Gibson, and R. M. Fleming, *Phys. Rev. B* **26**, 184 (1982).
- ²²X-Q. Pan, M-S. Hu, M-H. Yao, and D. Feng, *Phys. Status Solidi A* **92**, 57 (1985).
- ²³G. Van Tendeloo, J. Van Landuyt, P. Delavignette, and S. Amelinckx, *Phys. Status Solidi A* **25**, 697 (1974).
- ²⁴G. Van Tendeloo, R. DeRidder, and S. Amelinckx, *Phys. Status Solidi A* **27**, 457 (1975).
- ²⁵W. L. McMillan, *Phys. Rev. B* **14**, 1496 (1976).
- ²⁶A. Amelinckx, G. Van Tendeloo, and J. Van Landuyt, *Phys. Scr. T* **25**, 34 (1989).
- ²⁷M. Onoda, M. Sera, K. Fukuda, S. Kondoh, and M. Sato, *Solid State Commun.* **66**, 189 (1988).
- ²⁸H. Krakauer and W. E. Pickett, *Phys. Rev. Lett.* **60**, 1665 (1988).
- ²⁹Y. Matsui, H. Maeda, Y. Tanaka, E. Takayama-Muromachi, S. Takekawa, and S. Horiuchi, *Jpn. J. Appl. Phys.* **27**, L827 (1988).

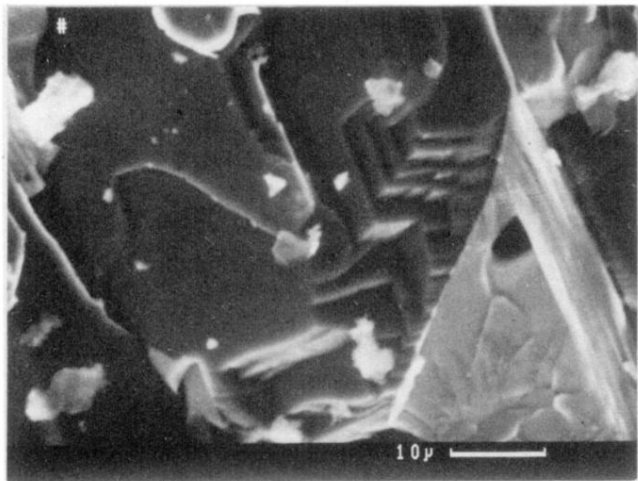


FIG. 1. SEM micrograph of fractured sample *B*.

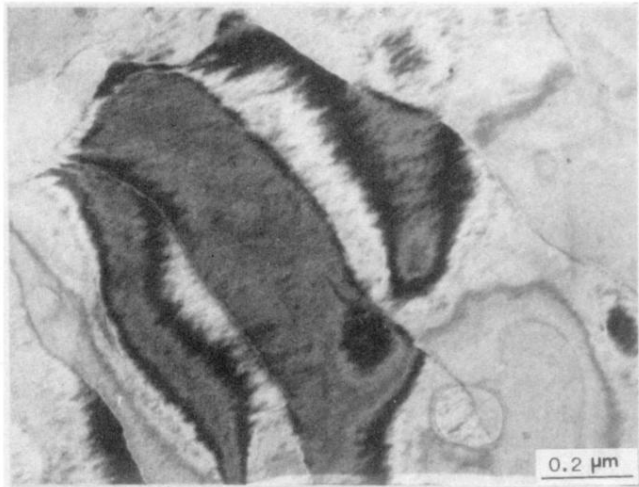


FIG. 2. BF image of sample *A* (zone axis (*z*) = near[001]).

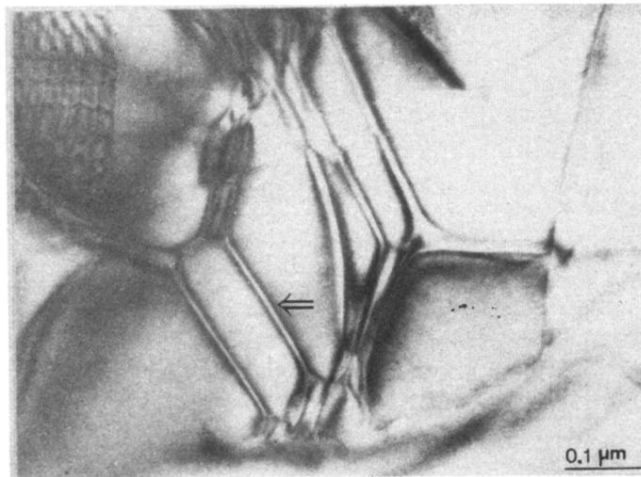


FIG. 3. BF image of sample C.

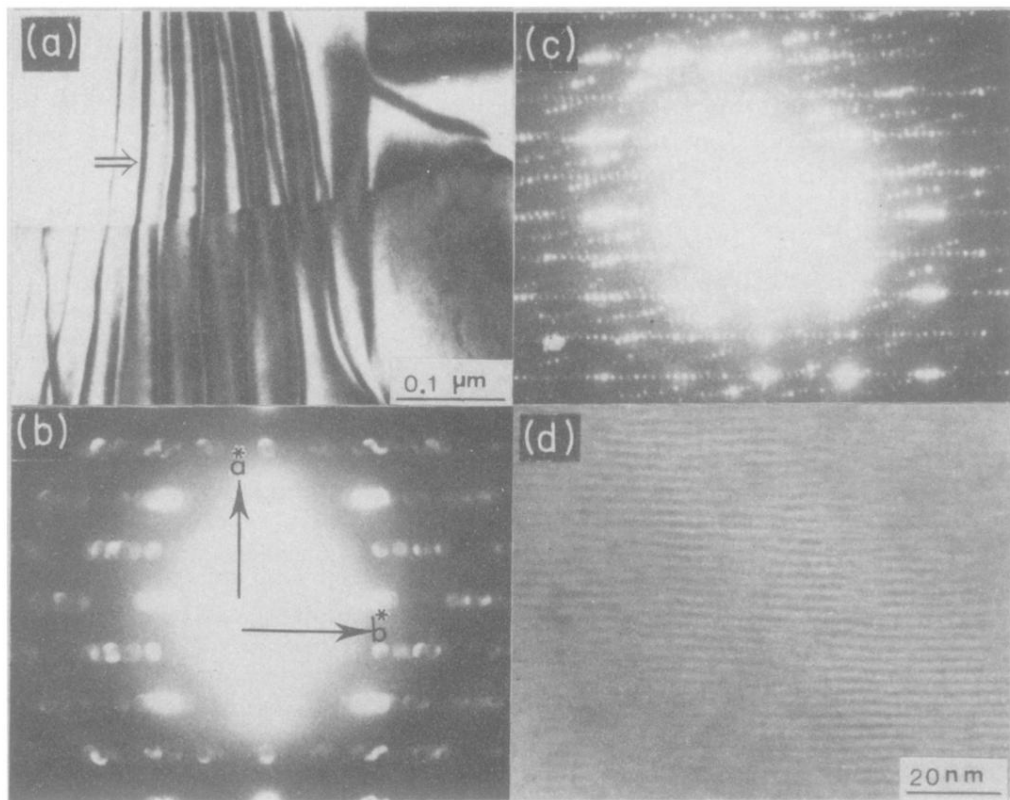


FIG. 4. BF image of sample *B* (a) together with its CBED (b) and SAD (c) patterns as well as Moiré image of a stripelike line (d).

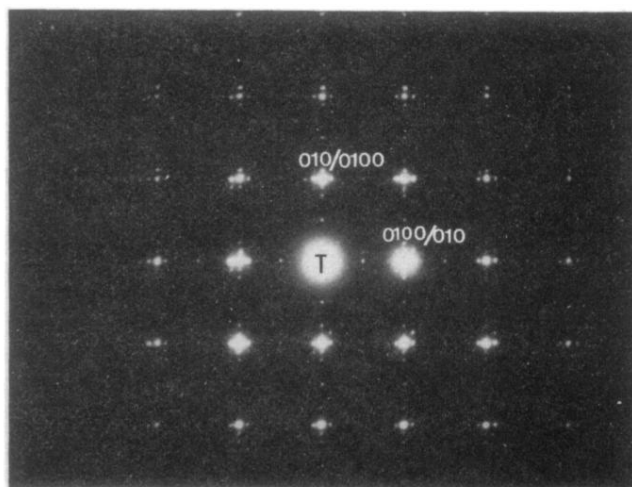


FIG. 5. A representative SAD pattern for a 90° twist boundary on sample C.

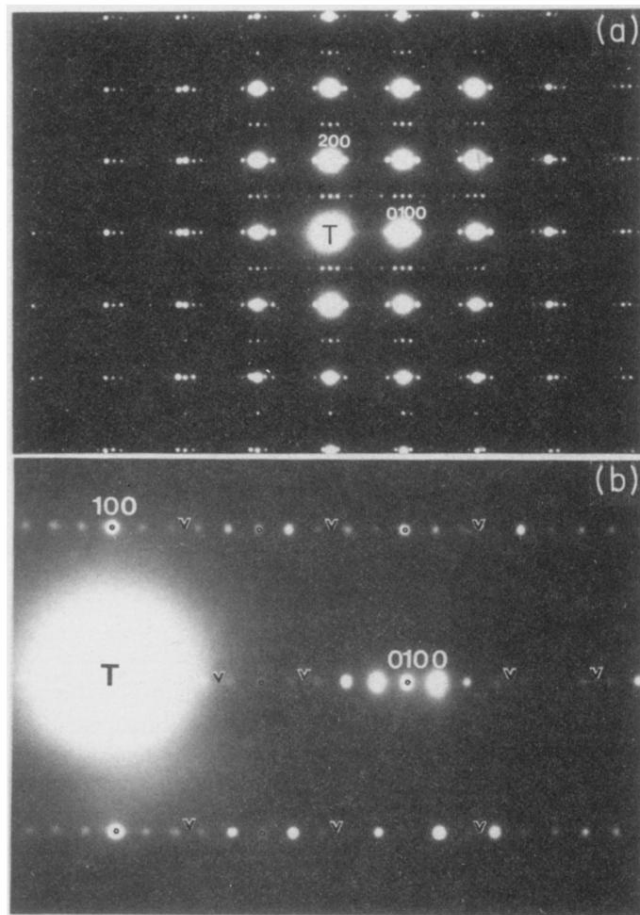


FIG. 6. SAD pattern of sample *C* (z =near $[001]$) (a), together with its enlarged pattern (b).

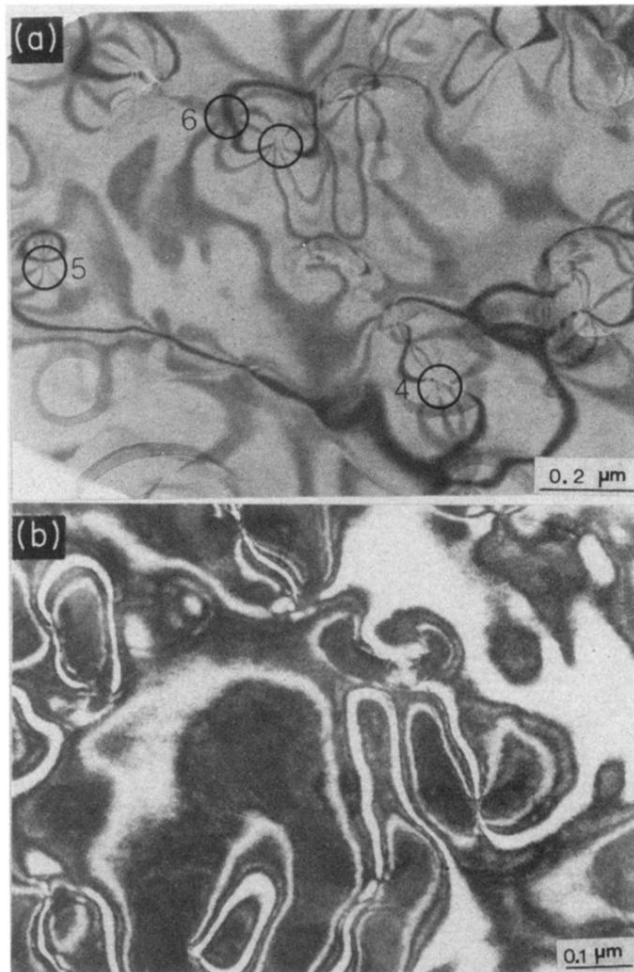


FIG. 7. BF (a) and DF (b) images of sample C, which were obtained at $z = \text{near}[001]$.

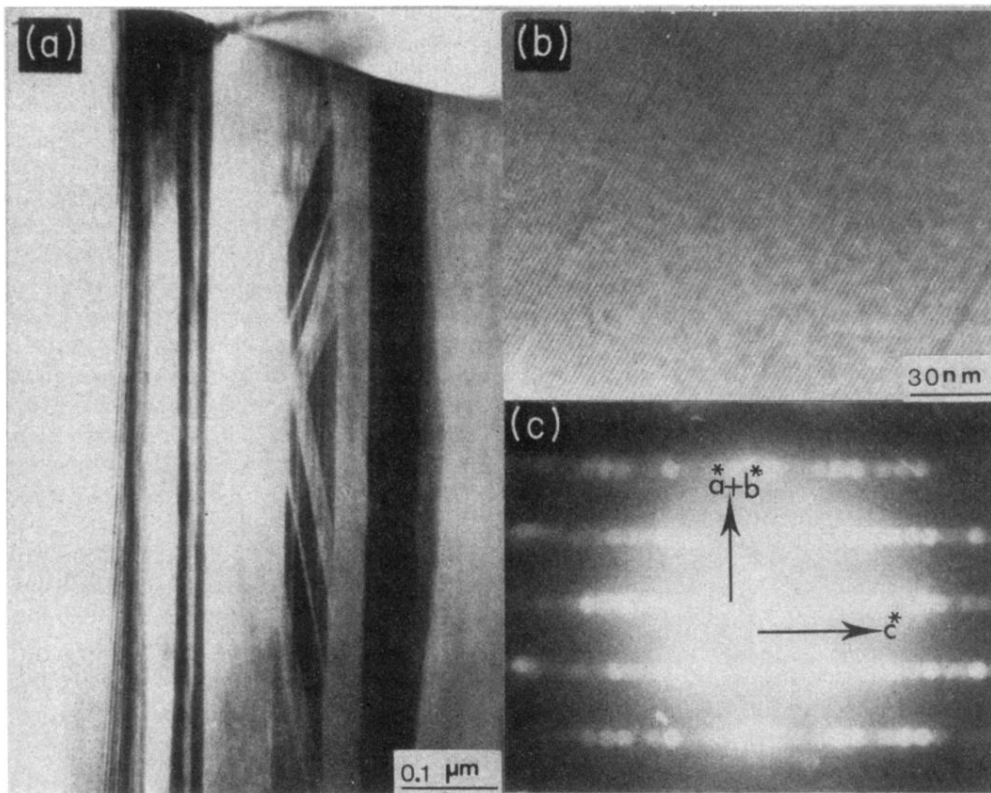


FIG. 8. BF image of twins (a) on sample C together with its HREM image (b) and SAD pattern (z =near $[5\ 10\ 0]$) (c).